WHAT COULD HAPPEN IF THE PARBUCKLING OF COSTA CONCORDIA HAD FAILED: ANALYTICAL AND CFD-BASED INVESTIGATION OF POSSIBLE GENERATED WAVE

Alberto Lamberti[1], Alessandro Antonini[2] and Giovanni Ceccarelli[3]

Costa Concordia is well known throughout the world as the ship which partially sank after a collision with rocks near to Giglio Island. The successful parbuckling operation has received wide coverage from the media. The estimated presence of hundreds of persons, journalists and tourists near the location of the partially sank ship during the recovery operations required an estimation of which wave could be generated if any malfunctioning might occur and the vessel might fall down into the water with its huge mass. Due to the short time between the analysis require and parbuckling start-up, a quick estimation of the possible generated wave was carried out. The present contribution aims to verify the accuracy of the estimation by comparison with a state of the art numerical simulation. A CFD simulation of the vessel partially emerged falling into the water has been done. Different configurations of the wreck positions at failure and different failure modes are investigated in order to identify the worst scenario.

Keywords: Costa Concordia; parbuckling; motion equation; CFD; STAR-CCM+

Introduction and objectives

Costa Concordia was a cruise ship which was wrecked off the coast of Giglio Island in Italy on 13 January 2012. On that day, Costa Concordia struck a rock in the Tyrrhenian Sea just off the eastern shore of Giglio Island, on the western coast of Italy. Such event tore a gash on the port side of her hull, resulting in power loss to her propulsion and electrical systems. With water flooding in, the ship drifted back to Giglio Island where she grounded 500 m north of the village of Giglio Porto, resting on her starboard side in shallow waters with most of her side under water, Fig. 1.

Figure 1. The grounded wreck of Costa Concordia (Ceccarelli 2013)

It was announced in May 2012 that the American salvaging firm Titan Salvage and Italian underwater construction firm Micoperi had won the salvage contracts following competitive bidding, (The Guardian 2012). The Titan-Micoperi salvaging plan included the five following operations, (Ceccarelli 2013), Fig. 2:

1. Stabilization: this phase involves the anchoring and stabilization of the wreck to prevent any slipping or sinking along the step seabed by means of retaining cables that hold the wreck at its base.
2. Parbuckling preparation: the phase involves the preparation of the underwater support on which the wreck rests after rotation. After the realization of this structure, the re-floating portside sponsons are installed and the retaining strand are tensioned from jacks placed on towers.
3. Parbuckling: several cables attached to the underwater support are pulled by strand jacks placed on the top of sponsons, while the retaining cables hold the wreck at its base. At the end of this phase the sponsons are flooded until the wreck reaches the support structure.
4. Refloating preparation: further refloating sponsons are attached to the starboard side of the wreck. These sponsons are used during the refloating phase.

[1] DICAM, University of Bologna, Via Risorgimento 2, Bologna,40136, Italy. e-mail: alberto.lamberti@unibo.it
[2] DICAM, University of Bologna, Via Risorgimento 2, Bologna,40136, Italy. e-mail: alessandro.antonini2@unibo.it
[3] Engineering Manager Titan Micoperi, via Ignazio Sarti 7, Ravenna, 48121, Italy.
e-mail: gceccarelli@ceccarelliyachtdesign.com

5. Refloating: the sponsons are gradually emptied giving the sufficient shove to push the wreck upwards until reaching floating condition, then the ship is towed to demolition yard.

The present work concerns only the effects, in terms of generated wave, of three possible malfunctionings that could happen during the parbuckling phase.

Part of the following study, the analytical one, was requested us directly by Titan-Micoperi; it aimed to provide an evaluation of the height of the waves that may be generated by any malfunctionings during parbuckling of the Concordia wreck in order to outline the potential impacts of the operation on the surrounding environment. Due to short time (a week-end) assigned before parbuckling start, a quick estimation of the possible generated wave was made by means an analytical solution, while later a CFD analysis of the generated wave has been completed in order to verify the accuracy of the quick estimation by means of comparison of results. In this paper both the methods are described and their results are compared in order to highlight the accuracy of the analytical model by comparison with results of the more realistic CFD simulations.

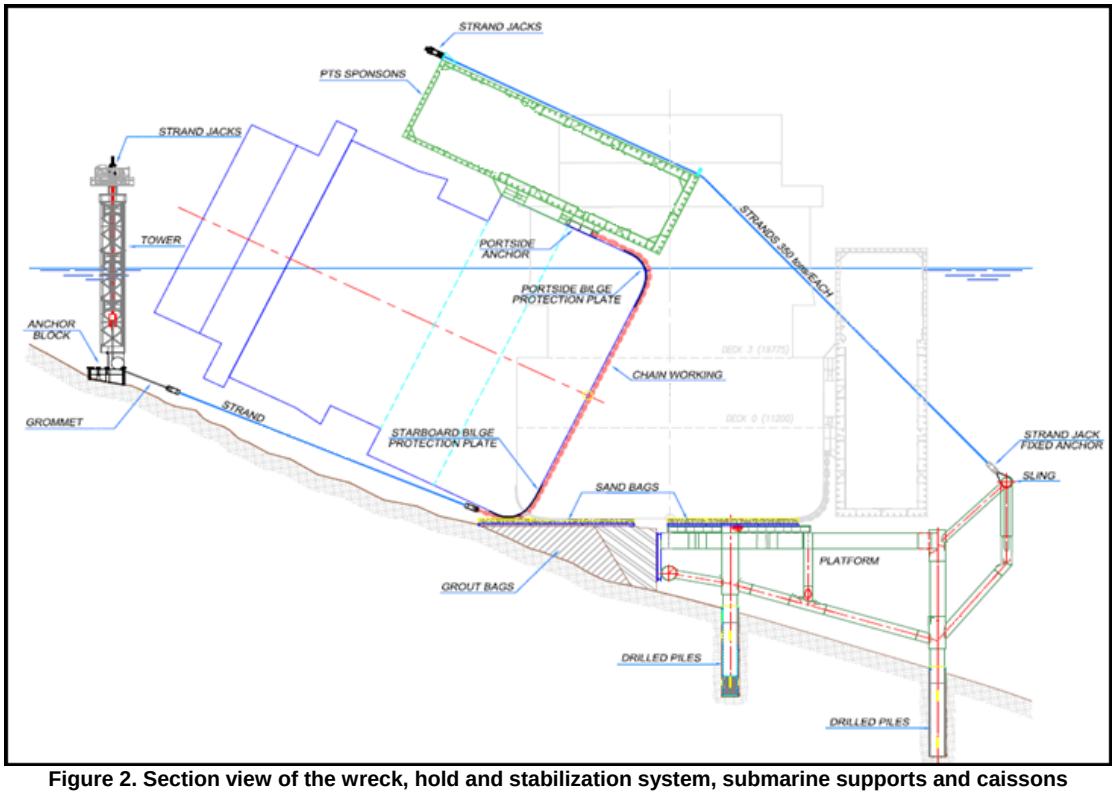

Figure 2. Section view of the wreck, hold and stabilization system, submarine supports and caissons (Ceccarelli 2013)

Considered failure modes

A similar study was conducted by D'Appolonia before the stabilization phase, to outline the risks that may result from slipping of the wreck along the steep seabed, from the depth of 30 m to the slope base at 90 m depth, (D'Appolonia 2012). After the completion of the stabilization works, the sliding of the wreck towards deep water does not represent a likely event since it would require the combined failure of retaining cables and supporting structures.

The following scenarios are considered:

1. simultaneous failure of all the portside pulling cables during the initial phase of parbuckling, i.e. before reaching the top dead center (the center of gravity lies along the vertical passing through the rotation axis) with the consequent fall of the wreck towards the island, Fig. 3;

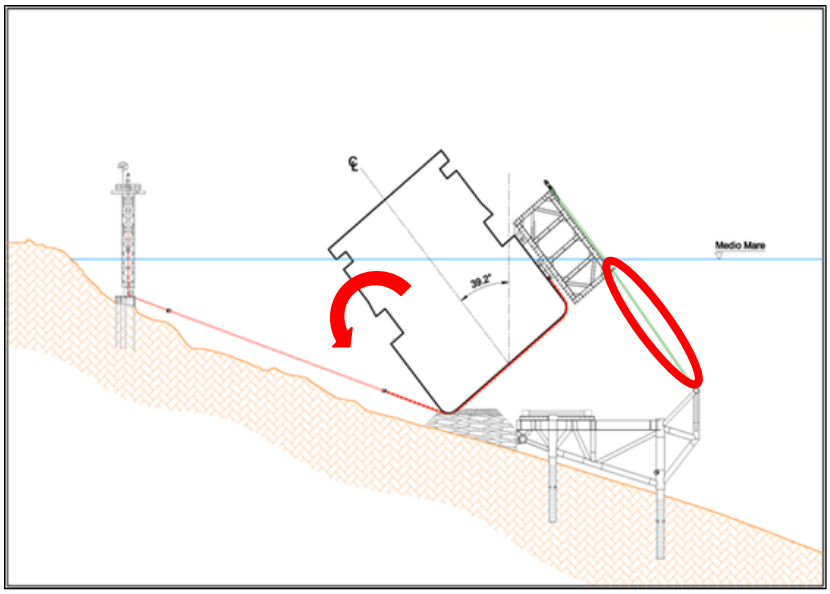

Figure 3. First failure scenario

2. failure during the initial phase of parbuckling, of the retaining cables that hold the wreck at its base on its starboard side, with the consequent fall of the wreck towards the island, Fig. 4;

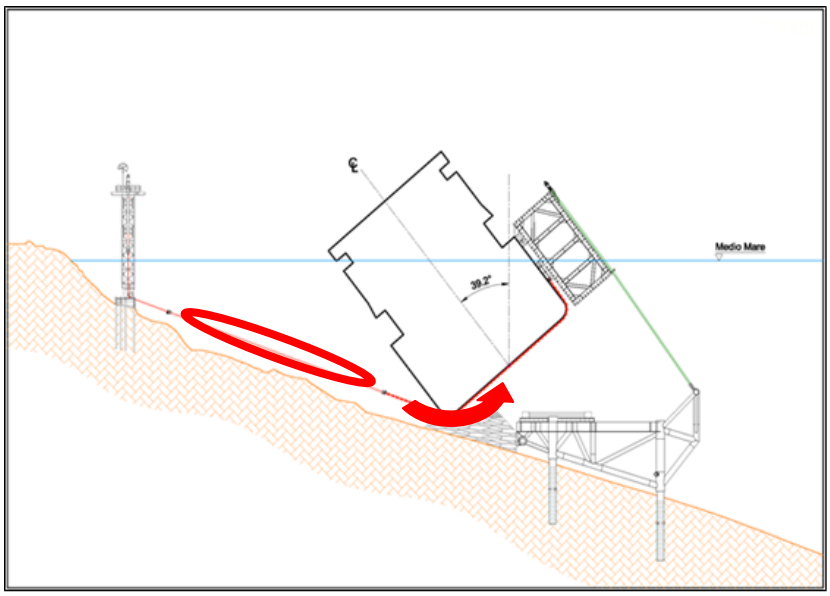

Figure 4. Second failure scenario

3. failure of the portside sponson connections, after passing the top dead center, with the consequent uncontrolled parbuckling of the wreck falling on the support structure, Fig. 5.

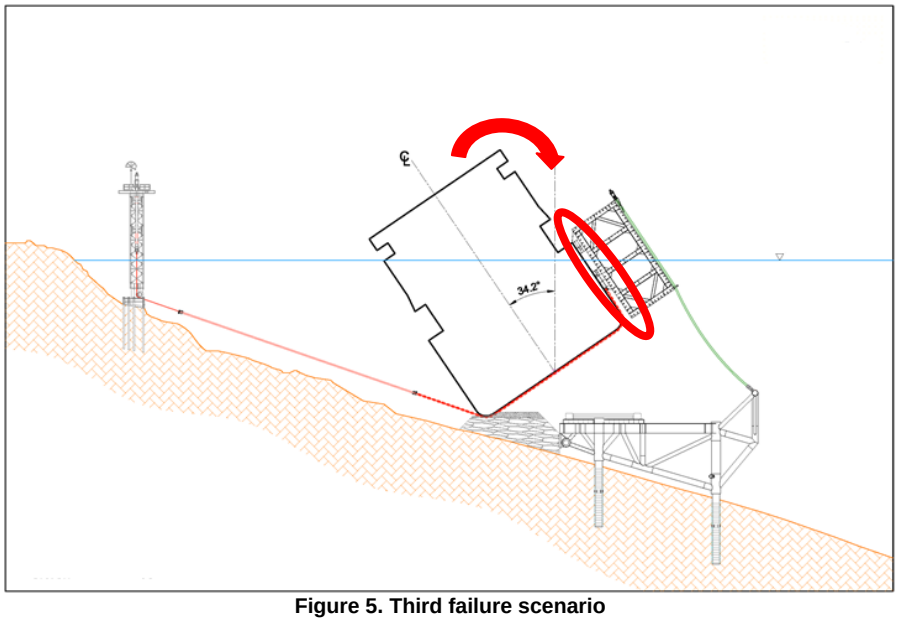

Figure 5. Third failure scenario

For all the failure scenarios the defect of resistance to the nominal workload values can be excluded since all the elements were separately tested for these conditions. Failures may occur due to unpredicted eccentricity of the masses in the wreck or because the wreck might be hooked into rocks causing an anomalous conditions requiring untested workload.

Wreck details and position of the center of gravity

The survey of the natural condition shows that the wreck lies on two granitic prominences. The wreck leans on the prominences at a depth of nearly 30 m where the seabed has an inclination of almost 25°. The wreck is partially sunken and leans on its starboard side with an inclination of almost 65°. The principal dimensions of the wreck are shown in Table 1.

Table 1. Vessel details	**Values**
Length over all	290.0 m
Length between perpendiculars	250.0 m
Breadth	38.0 m
Draft (summer load)	8.3 m
Operating Displacement	55’000 t
Wreck details	**Values**
Wreck weight, tilt angle 65° (pre-parbuckling)	45’000 t
Sponson, Blister, Strand jack weight	8’700 t
Wreck buoyancy force (void fraction 97 %)	16’200 t
Sponsons buoyancy force	4’000 t

The identification of center of gravity position was carried out by the company OVERDICK, different void fraction of the flooded body and center of gravity envelop were presented in the company studies, but for this study only the most heavy case was adopted. This assumption leads to select the results related to value of void fraction to 97 %, in Table 2 the related coordinates are shown, (OVERDICK 2012).

Table 2. Weight and position of the center of gravity for flooded compartments and hull

Axis X: from aft perpendicular pointing towards bow
Axis Y: from Center Line (CL) pointing towards portside
Axis Z: from Base Line (BL) pointing upwards

Item	Weight [t]	Xc [m]	Yc [m]	Zc [m]
Hull	54048.8	115.9	2.9	17.0
Flooded compart.	252814.9	120.3	-4.1	20.3
Total	306862.9	119.5	-2.9	19.7

Analytical method

The accurate evaluation of the wave produced by some malfunctionings in the parbuckling operations would require an equally accurate evaluation of the dynamics of the wreck, including the movements of the water inside it, of the friction on the seabed and of the wreck-water interaction, both in terms of mass moving inside the wreck and outside it (local stationary oscillations and added mass) and in terms of perturbations that propagate irradiating energy. Considering all the above mentioned terms leads to a complex theoretical approach, which would not have been solved in the short assigned period, therefore a simplifying hypothesis on the falling process has been adopted.

The falling process from initial static condition is limited, at the beginning, by inertia which contrasts rapid changes of velocity, and then, after a significant time, by hydrodynamic damping increasing with velocity, that causes its asymptotic and not exceeded value, that we can easily calculate by neglecting inertia.

In the first case falling velocity of the wreck is evaluated, neglecting added mass, friction on the seabed, and the force due to generated wave. All these components contribute to increase falling time and to reduce speed and the intensity of fall effects. This evaluation only provides a first upper limit for the height of the generated wave that is reliable in the initial phase of the fall.

In the second case, wave generated by the wreck movements is evaluated with the most simple method: 2D wreck motion, 2D wave propagation on flat bottom according to shallow water approximation, which assumes pressure from the wave and velocity on the vertical line to be constant. The asymptotic fall velocity is reached when the wave force equates the wreck lack of balance.

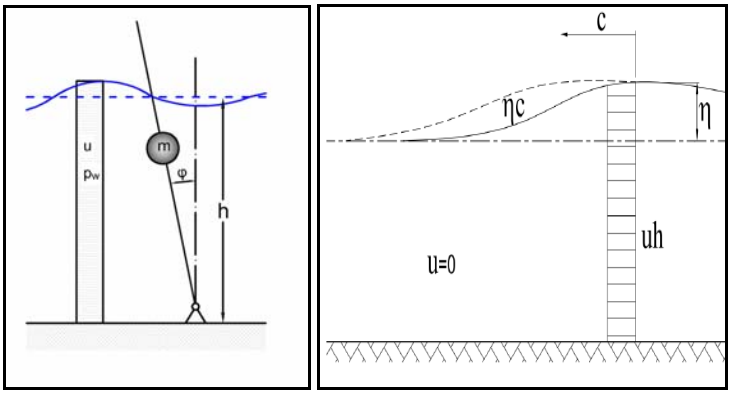

Figure 6. Schematic view of the adopted approximation, *u* is the horizontal water particles velocity, p_w is the pressure due to the wave, *m* is the mass of the wreck, *h* is the depth, *φ* is the rotation angle, *η* is the surface elevation and *c* is the wave celerity.

Furthermore, for a progressive wave formed on still water, free surface elevation η, wave celerity c, water depth h, velocity u and discharge per unit width q are linked by the following simple relation which can be derived from water volume conservation and simple wave propagation equation on initially immobile water body, Eq 1.

$$\frac{\partial \eta}{\partial t} + \frac{\partial q}{\partial x} = 0$$
$$\frac{\partial \eta}{\partial t} + c \cdot \frac{\partial \eta}{\partial x} = 0 \qquad \Rightarrow q = c \cdot \eta = u \cdot h \tag{1}$$
$$u = 0 \quad \text{when} \quad \eta = 0$$

The water that surrounds the wreck is divided into starboard water and portside water, the generated perturbation will show different behavior for each side. The waves will leave the wreck following different directions as well as the generated discharges and pressures which will have different values and signs according the wreck side. Thus the water rises on the side where the wreck is falling while a depression propagate on the opposite side; both the generated wave forces work together in contrasting the wreck rotation.

Under these hypothesis, considering the imbalance of forces which generates the movement of the falling wreck, the amplitude of the perturbation for which the hydrodynamic brake (*d*) equals the existing imbalance of forces can be evaluated, Eq. 2.

$$d \cdot \dot{\varphi} = M \tag{2}$$

Moreover, knowing the displaced volume wreck falling angle relation Eq 3, the height of the wave can be easily found and so the wave pressure that, assuming the approximation of shallow water to be correct, is constant on the vertical line, Eq 4. Where b is the length of the equivalent wave generating paddle.

$$q = \frac{1}{2} \cdot b \cdot \dot{\varphi} \tag{3}$$

$$p_w = \rho \cdot g \cdot \eta \tag{4}$$

From Eq 4, by integrate along the vertical, resistance to rotation or translation due to surrounding water can be evaluated and consequently the related perturbation amplitude, Eq 5.

$$\eta = \frac{1}{2 \cdot c} \cdot h \cdot \dot{\varphi} \tag{5}$$

Inertia and hydrodynamic resistance act together in counteracting the acceleration. The two extreme case solutions, neglecting one of the limiting factors, are both approximations of the real value, both the solutions can be considered and thus only the least unfavorable be used as it will be shown in scenario 1.

Analytical method: scenario 1, simultaneous failure of all the portside retaining cables

In case of yielding of all the retaining cables the wreck would rotate towards the island expelling the water between the starboard side and the seabed on one side and drawing water on the opposite side. If the retaining cables yield during the first phases of the parbuckling, the inertia of the wreck would not allow the development of the falling velocity and consequently also of significant waves. Considering the first approach described above, neglecting the resistance to fall offered by the waves, and taking into account the inertia of the wreck, the falling velocity of the wreck and the time to reach the seabed can be estimated. The evaluations made by Overdick (OVERDICK 2012) for Titan-Micoperi highlight at the end of a fall with a duration of 14 seconds, a maximum angular velocity of 1,9 °/s; this rotation would create a discharge of almost 30 mc/s/m towards the island and a wave crest of 1,7 m while a discharge of almost 20 mc/s/m in the opposite direction with a wave trough of 1,2 m which will propagate towards the open sea. As the fall proceeds, the moment of the weights increases until the velocity reaches the asymptotic value (second approach), ending in generated waves, of 1.60 m wave crest toward the island and 1.10 m wave trough propagated towards the open sea, corresponding to a velocity of rotation of 1.7 °/s.

Analytical method: scenario 2, failure of the retaining cables that hold the wreck at its base

22 retaining cables, passing under the wreck and fixed to its port side guarantee the stability of the wreck on the starboard side. The retaining cables are tightened by as many strand jacks installed outside of the water on turrets Fig. 2. If the friction between the wreck and the seabed is constant and

able to prevent slippage of the wreck towards the open sea, the load acting on the retaining cables would be equal to 0 also for a shift of a few cm, not enough to create significant waves. On the other hand, if the slip, even if small, causes a significant reduction in the friction between the wreck and the seabed, a part of the current frictional force (component of the weight along the seabed which is around 15'200 t) may be lost. In order to generate a value of load on the cables of the holdback system equal to the design load around 11'000 t, the friction factor, after the first movement, has to decrease to values of almost 0.10 (while 0.45 corresponds to the balance without holdback system). In this case the sliding speed, which determining a resistance due to the generated wave equal to the lost force of the holdback system, would be 0.42 m/s, thus creating a wave crest of 0.75 m on the port side and a similar depression on the starboard side.

Analytical method: scenario 3, failure of the portside sponsons

During the descent phase from its top dead center the wreck is prevented from auto rotating by the buoyancy of the sponsons, while the pulling cables are maintained in tension to prevent rolling of the wreck and to maintain the control on its movements. The weight of the wreck and the pulling of the cables are balanced by the buoyancy force of the sponsons. In this phase, if the procedures are performed correctly, the two moments with respect to the center of rotation reach the maximum intensity of 2.6×10^6 kNm when the parbuckling is completed while for a 10° inclination the imbalance reduces to 1.7×10^6 kNm. Assuming this last value as the hydrodynamic resistance developed by the generated wave, we can deduce a wave crest equal to 1.10 m towards the open sea and a depression of 0.45 m towards the island, corresponding to a discharge of 9.9 mc/s/m in the same direction.

CFD method

To predict the dynamic of the falling process more accurately, a comprehensive study of the wreck motion that considers nonlinear interactions by using Computational Fluid Dynamics (CFD) methods can be adopted. CFD methods are widely used to model the complex nonlinear hydrodynamic of the wave structure interaction. In this study an unsteady RANS-based CFD model STAR-CCM+ is used (CD-Adapco 2013), where the governing equations are discretized over a computational mesh using a finite volume method. The unsteady incompressible flow field is described by the continuity equation and the Navier–Stokes equations Eq 6,

$$\begin{aligned} \nabla \cdot \mathbf{U} &= 0 \\ \rho \cdot (\mathbf{U}_t + \mathbf{U} \cdot \nabla \cdot \mathbf{U}) &= -\nabla p + \mathbf{F}_b + \nabla \cdot \mathbf{T} \end{aligned} \tag{6}$$

where ρ is the water density, $\mathbf{U}$ is the flow velocity vector and $\mathbf{U}_t$ is its time derivative, $\mathbf{F}_b$ is the body force vector (e.g. gravity), and $\mathbf{T}$ is stress tensor. A k–ω SST turbulence model is applied with a two-layer all y^+ wall treatment model, and a second order implicit scheme was used for time marching as suggested by Yu, (Yu 2011).

The transient SIMPLE algorithm is applied to linearize the equations and to achieve pressure–velocity coupling. A volume of fluid method (VOF) is applied to capture the free surface, and a overset mesh model is adopted to follow the movements and adjust the grids around the wreck due to its dynamic motion. Note that the equation of motion calculation is coupled with the flow field simulation through iterations. The equation of motion is solved within the SIMPLE algorithm, where the dynamic response of the floating body is calculated by integrating (over time) the acceleration obtained from the equation of motion solution using an implicit algorithm. The body is then moved to a new position and the movable part of the mesh is updated.

The convergence of the coupling between the RANS simulation and the dynamics of the body is reached at each time step. The dynamic motion of a floating-body is described by the equation of motions Eq 7,

$$\begin{aligned} m \cdot \mathbf{a} &= \mathbf{F} \\ \mathbf{I}_g \cdot \mathbf{a}_\Omega + \boldsymbol{\Omega} \times \mathbf{I}_g \cdot \boldsymbol{\Omega} &= \mathbf{M} \end{aligned} \tag{7}$$

where m is the mass of the unitary wreck slice and the water mass in the flooded compartments, $\mathbf{a}$ is the acceleration vector for the translation, $\boldsymbol{\Omega}$ and $\mathbf{a}_\Omega$ are the angular velocity and the acceleration vector, $\mathbf{I}_g$ is the moment of inertia tensor at the slice center of gravity, $\mathbf{F}$ and $\mathbf{M}$ are the total force and

moment vector acting on the wreck slice. As the selected failure modes predominantly operate in roll, the wreck motion is limited to a single degree of freedom (roll) motion. Eq.7 is then reduced to one degree of freedom equation. As a result, the equation of motion in roll for the wreck became Eq 8:

$$I_g \cdot a_\Omega + \Omega \times I_g \cdot \Omega = M_z \quad (8)$$

where M_z is the moment component in roll.

Slice wreck dimensions, domain and boundary condition

Fig. 7 shows the geometry of wreck slice used in the numerical tank test and the surrounding domain. In the RANS simulation, is considered only a basic structural design, where the wreck model geometry neglects the chimney appendix and the details of the sides of the boat. In order to identify total mass and inertia moments of the equivalent unitary section, mass of the hull, mass of the water inside the hull considering void ratio equal to 97 %, (OVERDICK 2012), mass of sponson and sponson's ballast, are mediated along the total length of the solid adopted to schematize the whole wreck (250,0 m) and then used to calculate the characteristics of the simplified slice geometry. The mass of the full-scale body slice used in the RANS simulations was about 1227.5 t with the center of gravity located 10.3 m below the mean free surface as shown in Fig. 7.

The computational domain is 300 m long ($-60 \leq x \leq 240$), 1 m wide ($-1 \leq y \leq 0$), and 140 m high ($-90 \leq z \leq 50$). The side distance from the coast is limited by the real bathymetry, while the distance on the off-shore side is chosen in order to have as less as possible reflection from the outlet boundary. The seabed at the rotation point of the wreck is given at 30 m below the mean water surface while at the off-shore boundary is given at 90 m. A flat surface inlet condition is specified at the top boundary, the pressure outlet is implemented at the coast and off-shore boundaries, two symmetry boundaries are used to generate the unitary slice of wreck and domain, the bottom and the hull surface are modelled as a no-slip wall. To absorb the outgoing and reflecting waves without creating additional numerical disturbance, a sponge-layer method is applied (CHOI 2009), in which a damping zone (180 m in the off-shore wave propagation direction) is placed in front of the outlet boundary.

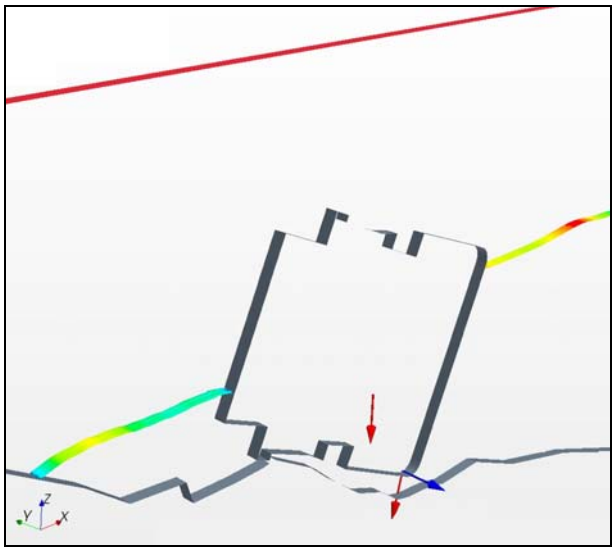

Figure 7. Wreck slice without sponson and bottom boundary

The meshes were created using the STAR-CCM+ grid generation utility. Fig. 8 shows the grid resolution around the Costa Concordia model. The grid resolution is finer near the free surface and around the wreck slice to capture both the wave dynamics and the details of the flow around the wreck. In addition, prism-layer cells are placed along the wreck surface, and the height of the first layer is set so that the value of y^+ satisfied the turbulence model requirement.

Using the overset mesh requires creating a background region, which is a closed surface solution domain, and one overset regions, which contain the physical movable body. The overset mesh is created using the overset mesh boundary, which is the outer boundary of the overset region that is coupled with the background mesh by means of linear interpolation. A critical factor in successfully applying overset meshes is to have enough cells across the overlapping zone between background and overset region. For this study the overlapping zone contains 5 cell layers in both background and

overset meshes. The horizontal grid size near the free surface Δx is determined by the wavelength identified by means of the analytical results, and the vertical grid size Δz is adjusted according to the wave height identified in the analytical method.

With regarding to the discretization of the domain, three volumetric controls are used: the first two (WS1, WS2 in Fig. 8) are aimed to improve the description of the free surface dynamic and are provided throughout the whole domain in the x direction, while the third one (O1 in Fig. 8) is aimed to generate the overlap region, has cylindrical shape with its axis passing through the rotation point of the wreck and a radius long enough to include the body during the falling process, equal to 55.0 m. Grid size of the volumetric control WS2 is chosen according Yu, who identified the convergence of the RANS simulation of a floating body, using values of discretization characterized by $\Delta x \leq \lambda/80$ and $\Delta z \approx H/20$, (Yu 2013). Volumetric control O1 has different features, it must guarantee homogeneity between the overset and background cells size, and at the same time, describe as better as compatible with the required time computing, the interaction between the surface of the wreck and the water. The characteristics for each volumetric control are summarized in Table 3.

Table 3. Characteristics grid size

Volumetric control	Length (m)	Height (m)	Δx (m)	Δz (m)
WS1	250	30	1.0	0.5
WS2	250	6	0.1	0.1
O1	Radius (m)		0.1	0.1
	55			

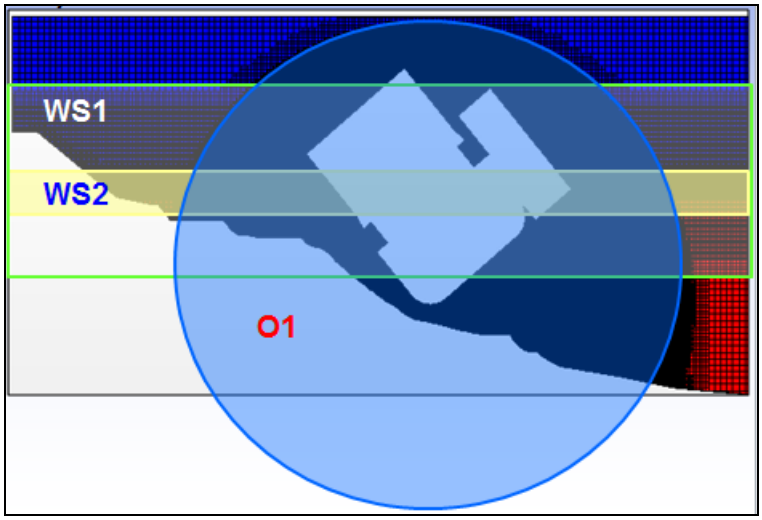

Figure 8. Domain detail and volumetric control for Scenario 1 and 2

CFD results

Both three scenarios were simulated in order to measure surface elevation generated by the motion of the wreck in terms of first crest and first trough propagated. Effectively the analytical analysis presented above was limited to, only, estimate the first perturbation which would be generated. Therefore, with the aim to compare the numerical results with the analytical ones the simulations are runned for 20 seconds. The measurements of the surface displacements are carried out by means of 6 wave gauges placed on both sides of the falling body. On the off-shore side of the wreck 5 wave gauges are used in order to applied a reflection analysis of the signal according to Zelt (Zelt 1992) and then exclude any reflection effects from the outlet region, whereas on the coast side only 1 gauge is used, Fig. 9. The main reason, the measurement requires more wave gauges on the off-shore side is the propagative nature of the off-shore perturbation, whereas the coast side perturbation is largely affected by the interaction with the steep bottom that forces the presence of stationary oscillation in front of the hull which cannot be interpret through the reflection analysis. Next paragraphs show the results of the simulations in terms of water surface elevation time series, highlight the peak reached by the first perturbation for both sides.

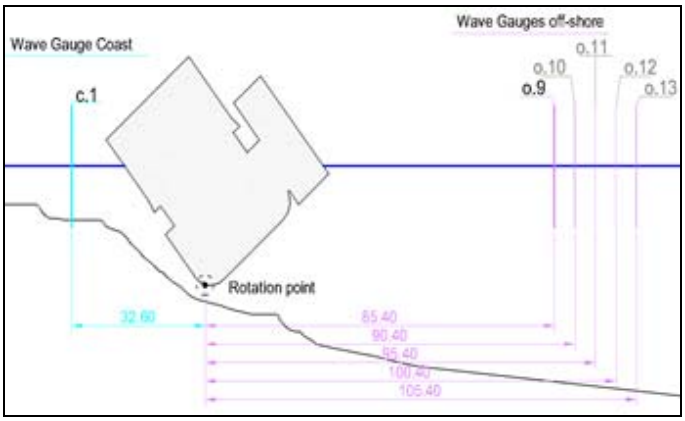

Figure 9. Wave gauges disposition

CFD method: scenario 1, simultaneous failure of all the portside retaining cables

In case of yielding of all the retaining cables the wreck would rotate towards the island expelling the water between the starboard side and the seabed on one side and drawing water on the opposite side. Simulation of this scenario is carried out imposing the rotation of the wreck around an unmovable axis coinciding with the lowest extreme of the hull and considering as initial position the maximum angle of rotation before the center of gravity oversteps the rotation point.

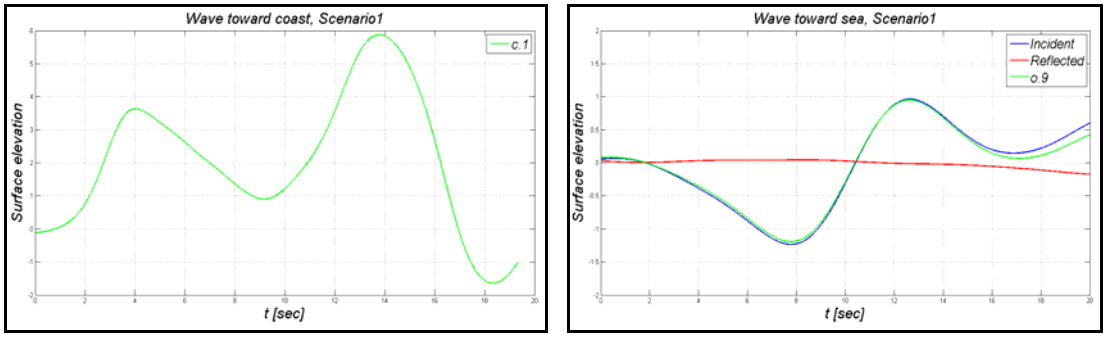

Figure 9. Free surface elevation for Scenario 1

Recorded signal on the coast side shows height of the first crest equal to 3.60 m which is discordant with the analytical results, Fig. 9. Such behavior is mainly due to the interaction with the bottom and the inability of the water to flow perpendicular to the rotation plane, both aspects were neglected during the analytical calculation leading to undervaluation of the crest height. The numerical solution can be considered affected by approximations as well as the analytical one, since the incapacity of the water to flow along the hull should be considered source of overestimation for the numerical solution.

The off-shore signal shows height of the first trough equal to -1.25 m, which better matches the analytical results, Fig. 9. Such matching of the results is due to the nature of the perturbation which is not largely affected by the interaction with the bottom and shows propagative nature which better match the interpretative model of the analytical description. Such kind of behavior will be found also for the scenario 3.

CFD method: scenario 2, failure of the retaining cables that hold the wreck at its base

22 retaining cables, passing under the wreck and fixed to its port side guarantee the stability of the wreck on the starboard side. The simulation regarding this scenario aims to reproduce the failure during the initial phase of parbuckling of the retaining cables with the consequent fall of the wreck towards the island. The simulation is performed imposing an unmovable rotation axis placed on the upper side of the sponson. The identification of such axis is carried out considering the intersection of the perpendicular line to the average slope of the bottom, passing for the contact point between the hull and the bottom, with the sponson upper surface, Fig 10.

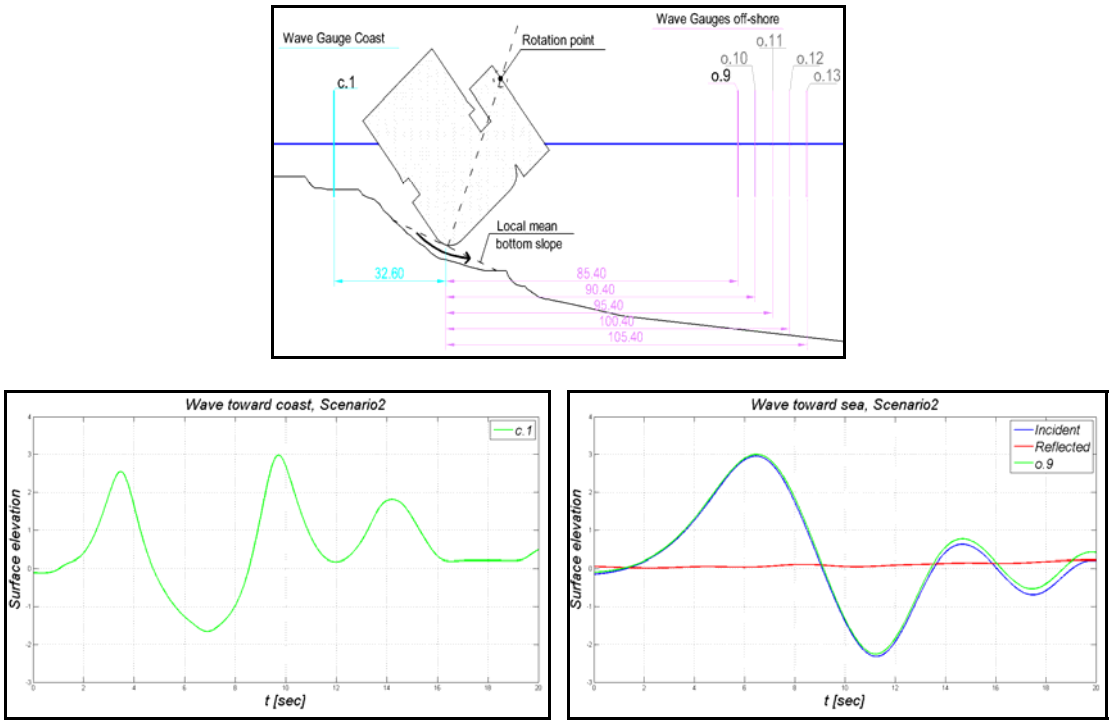

Figure 10. Rotation axis identification and free surface elevation for Scenario 2

This scenario is the only one to show a mismatch with the analytical results in terms of perturbation sign, such disagreement is mainly due to the approximation in the analytical model which neglect the shape of the falling body. It must be noted that during the process the hull shape is a major issue for the process since the water is pushed toward the bottom generating two water jets under the hull with the consequence of two wave crests propagated on both sides. In the analytical analysis, the falling body was modeled as a hinged flap which, inevitably, produce a perturbation of opposite sign at its sides. With regard to the intensity of the perturbation, the signal toward coast shows a crest equal to 2.55 m whereas a trough of - 0.75 m was calculated with the analytical method. The signal toward off-shore shows height of the first crest equal to 2.95 m which is much larger than the results identified above and equal to 0.75 m. Such mismatch can be imputable to the difference between the water velocity distribution imposed by the movements of the hull and the vertical distribution of the water particle velocities, characteristic of a propagative wave field, which reveals its effects producing large stationary oscillations affecting the wave field in front of the wreck.

CFD method: scenario 3, failure of the portside sponsons

During the descent phase from its top dead center the wreck is prevented from auto rotating by the buoyancy of the sponsons, while the pulling cables are maintained in tension to prevent rolling of the wreck and to maintain the control on its movements. The weight of the wreck and the pulling of the cables are balanced by the buoyancy force of the sponsons. In the case of the failure of the connections between the sponson and the hull surface the wreck would start an uncontrolled parbuckling. To model the scenario it is imposed an unmovable rotation axis coinciding with the lowest extreme of the hull and considering as initial position the minimum angle of rotation after the center of gravity oversteps the rotation point. Moreover the hull shape does not take into account the sponsons geometry, since we suppose absence of them during the rotation. Recorded signal on the coast side shows height of the first trough equal to -1.95 m which is discordant, in terms of amplitude, with the analytical results; whereas the first crest propagated toward off-shore is equal to 1.65 m which better match the analytical results, Fig. 11.

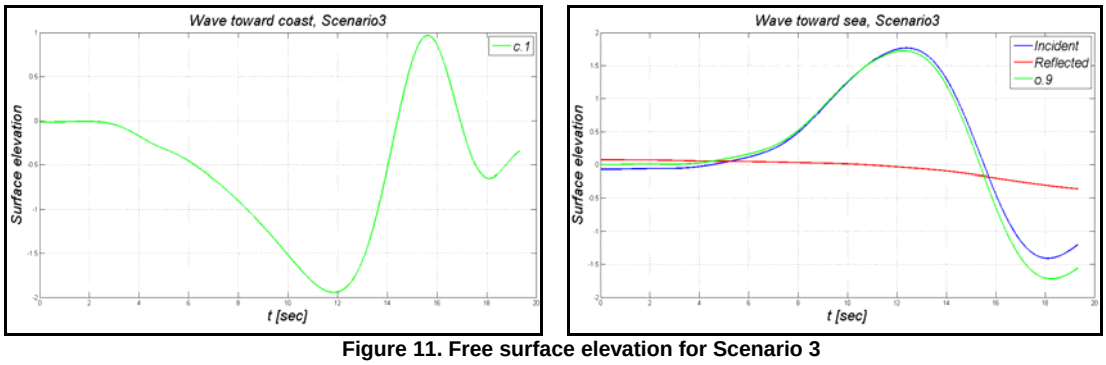

Figure 11. Free surface elevation for Scenario 3

CONCLUSION

In this work two different methods to estimate the possible generated wave due to possible malfunctionings of the parbuckling of Costa Concordia, are presented and discussed. The first one is based on the hypothesis of the shallow water and handles the falling wreck as a rotate hinged flap. Such method was used to estimate the possible generated wave approximately three days before the beginning of the parbuckling since no other approach could be applied given the short time assigned.

The second method aims to validate the analytical results via a CFD simulation developed in STAR-CCM+. The simulations are carried out according the overset mesh technique that allows to adopt different meshes for the background and for the movable body region in order to have only a restricted part of the numerical domain which follows the hull movements, avoiding any problems of reflection at the boundary due to the rigid rotation of whole discretized domain.

Both methods show strengths and weaknesses, and both results produced are approximation of the real nature of the phenomenon, but both are able to give an estimation of the amplitude of the perturbation that could be generated by the malfunctionings of the parbuckling. Comparison of the results are summarized in Table 4.

Table 4. Comparison of results

		Toward Coast	Toward off-shore
Scenario 1	Analytical	1.60	-1.10
	CFD	3.60	-1.25
Scenario 2	Analytical	-0.75	0.75
	CFD	2.55	2.95
Scenario 3	Analytical	-0.45	1.35
	CFD	-1.95	1.65

More in details, the analytical method was based on simplifications which allowed to estimate the order of magnitude of the possible generated waves in the short time assigned, but at the same time it showed some imprecision due to neglecting the wreck geometry. Furthermore, the values of perturbation estimated by means of such method can be considered valid in those cases where the waves radiating from the falling wreck, whereas the approximation gets worse when stationary modes or reflected waves are relevant since they could not be considered in the analysis.

With regarding to CFD simulations, the pseudo 2D numerical model shows higher values of perturbation amplitude since the generated wave cannot expand along the wreck axis, moreover, in the cases of coast side propagation, the amplitude is amplified by coastal reflection. The simulation of scenario 2 (which presents the worst matching between the results) was modeled as a rotation around a fixed hinge above s.w.l., such approximation induces stationary waves due to differences in water particle velocities distribution and the imposed distribution by the falling wreck. Such stationary oscillations are difficult to interpret through the reflection analysis adopted since they not have propagative nature.

To recapitulate, analytical estimation of waves did not take into account the local stationary oscillations since they are not propagative and then they are less influential for the surface elevation that could reach the harbor, where the spectators, the authorities and reporters were during the parbuckling operations. A common trend can be observed, CFD and analytical results are in agreement

for those perturbation propagated from the wreck toward the open sea, whereas the other direction of propagation showed some mismatch due to stationary and reflected waves.

Approximation on the hull shape adopted to analyze the fall in scenario 2 leads to large mismatch between numerical and analytical results, since the scheme used in the analytical method could not explain a wave generation characterized by the same sign for both sides of the wreck. Scenario 1 and 3 show good agreement between analytical and numerical solution obtained for the open sea side validating the results obtained before the beginning of the parbuckling.

REFERENCES

The Guardian. 18 May 2012. Costa Concordia salvage team prepares for "largest refloat in history". *The Guardian*. Accessed 11 Sept. 2014.

Ceccarelli, G. 2013. Rimozione del relitto della Concordia : il progetto ingegneristico e la realizzazione del raddrizzamento, *Studi di Aggiornamento sull'Ingegneria Off-Shore e Marina AIOM 2013.*

D'Appolonia, 2012. Removal operations of Costa Concordia wreck near Giglio island (Grosseto): analysis of the impulsive wave propagation generated by wreck sliding.
Internal report, Doc.No. 12-343-H11. (in Italian)

OVERDICK. 2012. Costa Concordia wreck removal: hydrostatic assessment of parbuckling. *Internal document, Doc.No. TMCC-OV-REP-40-003-08,*

CD-ADAPCO, Star-CCM+ 8.04 User Manual, *CD-ADAPCO, 2013*.

Yu, Y.H. and Li, Y. A RANS simulation of the heave response of a two-body floating-point wave absorber, *Proceedings of the 21st International Offshore and Polar Engineering Conference,* (ISOPE 2011).

Yu, Y.H. and Li, Y. 2013. Reynolds-Averaged Navier-Stokes simulation of the heave performance of a two-body floating-point absorber wave energy system, *Computer & Fluid*,73 ,104 -114.

Choi, L, and Yoon, S.B. 2009. Numerical simulations using momentum source wave-maker applied to RANS equation model, *Coastal Engineering*, 56, 1043-1060.

Zelt, J. and Skjelbreia, E. 1992. Estimating incident and reflected wave fields using an arbitrary number of wave gauges. *Proceedings of 23rd International Conference on Coastal Engineering.*